SHORT THESIS FOR THE DEGREE OF DOCTOR OF PHILOSOPHY (PHD)

Investigation of lemur tyrosine kinase 2 (LMTK2) protein in neurodegenerative dementias

by János Bencze MD

Supervisors:
Tibor Hortobágyi MD
Dag Aarsland MD

UNIVERSITY OF DEBRECEN
DOCTORAL SCHOOL OF NEUROSCIENCE

DEBRECEN, 2020

Investigation of lemur tyrosine kinase 2 (LMTK2) protein in neurodegenerative dementias

By János Bencze MD

Supervisors: Prof. Dr. Tibor Hortobágyi MD, PhD, DSc
Prof. Dr. Dag Aarsland MD, PhD

Doctoral School of Neuroscience University of Debrecen

Head of the **Defense Committee**:	Prof. Dr. Miklós Antal, MD, PhD, DSc
Reviewers:	Prof. Dr. Klára Matesz, MD, PhD, DSc
	Prof. Dr. Dániel Bereczki, MD, PhD, DSc
Members of the Defense Committee:	Dr. Péter Diószeghy, MD, PhD
	Dr. Attila Valikovics, MD, PhD

The PhD Defense takes place at the Lecture Hall of In Vitro Diagnostics Building, Faculty of Medicine, University of Debrecen
10:00 a.m. 24th of July, 2020

1. Introduction

Dementia is characterized by progressive cognitive decline severe enough to interfere the patient's everyday life such as ability to work or social relations. Alzheimer's disease (AD) and dementia with Lewy bodies (LBD) are the two most frequent neurodegenerative dementias affecting millions of people worldwide. Hallmark pathological features of AD are extracellular senile plaques containing abundant amyloid-β peptides and intracellular neurofibrillary tangles (NFT) formed by excessive amount of hyperphosphorylated tau protein. Therefore, we refer to AD as a tauopathy. Contrary, DLB belongs to the α-synucleinopathies, because of the excessive deposition of pathologically aggregated α-synuclein protein, which is detectable in the intracellular Lewy bodies and Lewy neurites. Although, there are several major differences between the pathogenesis of the disorders, neuropathological examination often reveals coexisting AD-type pathological changes in DLB, while 'pure' DLB is relatively rare. Imbalance between the production and clearance of intraneuronal proteins has a key role in the complex pathomechanism of the neurodegenerative disorders. Despite the comprehensive experiments, our knowledge on the processes leading to neurodegeneration is still insufficient. Thus, it is not surprising that AD and DLB are incurable diseases, only supportive therapy is possible. There is a growing pressure on the scientists to provide novel therapeutic targets by mapping the pathomechanism of neurodegenerative disorders.

Lemur tyrosine kinase 2 (LMTK2) was first described in 2002. This structurally unique membrane-anchored protein kinase is involved in several physiological (neuronal differentiation, intracellular vesicle trafficking, axonal transport, spermatogenesis) and pathological (prostate adenocarcinoma, lung cancer, cystic fibrosis) processes. Among the interacting partners of LMTK2 there are vital regulators of cellular functions such as cyclin-dependent kinase 5 (CDK5)/p35, catalytic subunit of protein phosphatase 1 (PP1C), cystic fibrosis conductance regulator (CFTR) or Kinesin-1, which is one of the major molecular motor proteins. LMTK2 has been comprehensively studied in malignant tumours, particularly in prostate cancer. However, our research group published the first scientific paper suggesting the LMTK2's role in neurodegeneration.

Based on cell biological and animal model studies, as well as on the interactome of LMTK2 we identified three potential mechanisms which may contribute to neurodegeneration under pathological circumstances: 1) tau phosphorylation, 2) apoptosis, 3) axonal transport. CDK5 the upstream regulator of LMTK2 and GSK3β, which is indirectly regulated by LTMK2 (via PP1C) are well-known major tau kinases. Their increased activity result in tau hyperphosphorylation. Apoptosis is an important mechanism of the neuronal cell loss often seen in neurodegenerative dementias. Decreased LMTK2-mediated inhibition on PP1C indirectly leads to pro-apoptotic processes via GSK3β overactivation. Disrupted axonal transport is one of the major impairments behind the intracellular accumulation of protein aggregates. Reduced LMTK2 activity results in GSK3β disinhibition, which in turn alters axonal transport by phosphorylation of the motor proteins.

Owing to that the number of human studies investigating the implication of LMTK2 in neurodegeneration is very limited, we obtained well-documented human AD, DLB samples and compared them to age-matched controls without dementia. Furthermore, we assessed samples with different neuropathological (Braak) AD stages in order to clarify the presumed connection between the expression of LMTK2 and the extent of AD-type NFT pathological changes.

We believe that LMTK2 will be a potential biomarker/drug target in the future. In that case, fast, valid, and easily reproducible detection of LMTK2 will be essential. Therefore, we used the widely spread, conventional immunohistochemical techniques in our work. However, data processing was executed with the most-modern digital image analytic solutions allowing us to process large amount of experimental data relatively fast. The scientific importance of our work is reflected by the facts that, on the one hand there is a special need for identifying novel neurodegenerative disease-specific biomarkers and on the other hand the presented work is the first description of LMTK2 in human neurodegenerative disorders.

2. Aims and scope

Neurodegenerative dementias are severe incurable diseases. Mapping the pathomechanism and identifying novel drug targets are of paramount importance for both diagnostics and therapy.

LMTK2 can meet these requirements, however the number of studies about its role in neurodegeneration is very limited. My main aim was to characterize the protein's complex pathophysiological role in neurodegenerative dementias. It should be noted that DLB is a clinical diagnosis, therefore in accordance with the neuropathological terminology we refer to the disorder as neocortical Lewy body disease (LBD) in the followFFings. During the PhD research work the main objectives were:

I) Histopathological characterization of LMTK2 in human post-mortem brain samples of patients suffered from neurodegenerative dementias.

II) Investigation of the LMTK2 alterations quantitatively, based on the intensity of immunohistochemical reaction, in the two most frequent neurodegenerative dementias, in Alzheimer's disease and neocortical Lewy body dementia, compered them to non-demented age-matched controls.

III) Clarifying the previously presumed connection between LMTK2 and tau-pathology in different brain regions and neuropathological (Braak) stages of AD.

3. Material and methods

3.1 Neuropathological characterization of LMTK2 in AD and neocortical LBD

3.1.1 Patients and samples

Three experimental groups were established: non-demented age-matched control (CNT), AD and DLB. In demented group we selected 6-6 AD and neocortical LBD cases with severe neurodegenerative changes (Braak stage VI and diffuse neocortical stage, respectively). Diagnosis of dementia was determined by the clinical symptoms ante-mortem and confirmed by post-mortem neuropathological examination. In the CNT patients there were no detectable neurodegenerative changes, they died in extra-neural diseases. The observed brain region was the middle frontal gyrus (MFG) which is severely affected in both disorders. We assessed the formalin-fixed paraffin-embedded (FFPE) samples of 11 females and 7 males. Every patient was older than 60 years, the average post-mortem delays were 38 hours (± 11.8 SEM) for AD, 47.1 hours (± 8.6 SEM) for CNT and 43.3 hours (± 7.8 SEM) for neocortical LBD cases.

All procedures were conducted under the ethical approval of the Institutional Ethics Committee of the MRC London Neurodegenerative Diseases Brain Bank (18/WA/0206) at the Institute of Psychiatry Psychology and Neuroscience, King's College London and the Brains for Dementia Research (BDR) Project (08/H0704/128+5). Informed consent for autopsy, neuropathological assessment and research participation were obtained from all subjects and data was anonymised.

3.1.2 Chromogenic immunohistochemistry (CHR-IHC)

7 μm thick FFPE sections were dewaxed in “decreasing” alcoholic concentrations. Endogenous peroxidase blocking was in methanol containing 3% (v/v) H_2O_2 for 30 minutes. Heat-induced epitope retrieval (HIER) was performed in Tris(hydroxymethyl)aminomethane - Ethylenediaminetetraacetic acid (TRIS-EDTA; 10mM TRIS Base, 1mM EDTA, pH 9.0) antigen retrieval buffer solution using microwave oven (5 mins. 800 watt, 2x5 mins. 250 watt). Non-specific antigen-binding sites were blocked in TRIS-buffered saline (TBS) with 10% (v/v) normal goat serum for 1 hour at room temperature. Sections were incubated with primary LMTK2 antibody (KPI-2 clone H-9, SantaCruz Biotechnology) overnight at 4°C. On the following day we incubated the samples with secondary goat anti-mouse biotinylated antibody (Agilent/Dako) for 1 hour at room temperature. IHC reaction was visualised by VECTASTAIN® Elite® ABC HRP Kit (Vector Laboratories). 3,3’-diaminobenzidine

tetrahydrochloride (DAB) reagent (Sigma-Aldrich 10mg tablets) was used for 4 minutes. Nuclear counterstain was haematoxylin. Sections were dehydrated in "increasing" alcoholic concentrations. Coverslipping was carried out by ClearVue™ Coverslipper (Thermo Fisher Scientific). Dilutions were 1:50 and 1:200 for primary and secondary antibodies, respectively. IHC negative slides (without the application of primary antibody) were also made for quality control purposes.

3.1.3 Fluorescent immunohistochemistry (IF-IHC)

Several steps overlap with the above detailed CHR-IHC protocol (dewax, HIER, primary antibody), others are not necessary for IF- IHC (endogenous peroxidase blocking, secondary antibody, DAB). Differences between the two techniques are the followings:

Working solution was phosphate-buffered saline (PBS; Biocare Medical, PBS Plus 10x solution, pH 7.3). Sections were incubated with fluorophore-conjugated secondary antibody (Goat Anti-Mouse IgG H&L – Alexa Fluor® 594, Abcam) in 1:200 dilution at room temperature for 1 hour. To avoid autofluorescence Vector® TrueVIEW™ Autofluorescence Quenching Kit (Vector laboratories) was used. Coverslipping was carried out manually with Vectashield® Antifade Mounting Medium with DAPI (4′,6-diamidino-2-phenylindole; Vector laboratories).

3.1.4 Assessment of CHR-IHC

Slides were scanned by Virtual Slide Microscope VS120 (Olympus Corp.) with the same illumination intensities, exposition times and camera settings. Cell-specificity, subcellular localisation and the connection between LMTK2 and disease-specific pathological changes (i.e. Aβ plaques and NFTs) were assessed by neuropathologist (TH).

3.1.5 Digital image analysis of IF-IHC

Fluorescent microscopy was performed with Axio Imager Z2 (Carl Zeiss AG) microscope with 20x/0,5 420350-9900 Ec Plan- Neofluar objective, Coolcube 1m S/N: 003274. 60N-C 1" 1.0x. 426114 camera and appropriate filter sets. Digital images were taken with Isis fluorescence imaging platform (MetaSystem Hard & Software GmbH). We took randomly 5 photos/cases at medium magnification (200x) using the same illumination intensities, exposition times and camera settings. Digital image analysis was executed with ImageJ software. Images were opened in one 'stack'. Threshold were 1-255 on greyscale. 'Erode' function was used to filter the edges of the neurons. In order to guarantee that every analysed object was neuron the

following filters were used: 1) size-based automatic selection, 2) manual selection to remove those object which were identified by the software but not neurons (i.e. blood vessels). Average greyscale intensities were determined by summarizing the measured values of the individual neurons. Then mean grey values were also calculated for the experimental groups (AD, CNT, neocortical LBD).

3.1.6. Statistical tests

Mean grey values of LMTK2 IF-IHC signals were analysed with SigmaPlot 12.0 (Systat Software Inc.). One-way analysis of variance (ANOVA) and pairwise Holm-Sidak method were executed. Furthermore, analysis of covariance (ANCOVA) was also run in order to clarify the influence of age at death or post-mortem delay on the results. SPSS 25 (IBM Corp.) software was used, dependent variables were IF-IHC results, fixed variables were, experimental groups and sex, while covariates were age at death and post-mortem delay.

3.2 Correlation between LMTK2 and tau-pathology

3.2.1. Patients and samples

Selection of cases based on the Braak tau neuropathological stages. We obtained 10-10 FFPE samples of 5-5 patients (n=10) with early (Braak I-III) and late (Braak VI) neuropathological stages of AD. Majority of the patients in the early neuropathological stage group had mild dementia. In the late neuropathological stage group, every patient suffered from severe dementia. Based on the spreading pattern of NFTs we selected two brain regions: 1) anterior hippocampus (aHPC) affected in both stages, 2) middle frontal gyrus (MFG), where NFTs are detected in late stage. Consequently, we established 4 experimental groups. In this setting MFG in early stage was the endogenous control region since it is not affected by NFTs.

All participants signed informed consent to participate in the study and to autopsy. The study was approved by the regional committee for medical and health research ethics in Western Norway (REK 2010/633); the Hungarian Medical Research Council, Scientific and Research Ethics Board (19312/2016/EKU); Institutional Ethics Committee of the MRC London Neurodegenerative Diseases Brain Bank (18/WA/0206) at the Institute of Psychiatry Psychology and Neuroscience, King's College London.

3.2.2 CHR-IHC labelling

7 μm FFPE sections were labelled with CHR-IHC techniques according to the previously discussed protocol in the *3.2.1* subparagraph. The only difference was the 1:100 dilution of primary LMTK2 antibody. This probably resulted from the subtle differences between the British and Norwegian pre-analytical tissue processing.

3.2.3 Fluorescent double-labelling immunohistochemistry (FDL-IHC)

Dewaxing, HIER, non-specific antigen binding sites blocking, preparation of primary LMTK2 antibody, blocking of autofluorescence and coverslipping were carried out by the methods discussed in *3.1.2* and *3.1.3* subparagraphs. LMTK2 was diluted in 1:100, the other used primary phospho-tau (Ser202, Thr205; clone AT8, Thermo Fisher) antibody was diluted in 1:500 concentrations in PBS. Fluorophore-conjugated 'fragment antigen-binding' (FAB) region (FabuLight™, Jackson ImmunoResearch Europe Ltd.) secondary antibodies were used. LMTK2 was labelled with red emitting (Alexa Fluor® 594 -AffiniPure Fab Fragment Goat Anti-Mouse IgG), while phospho-tau was labelled with green emitting (Alexa Fluor® 488 – AffiniPure Fab Fragment Goat Anti-Mouse IgG) secondary antibodies. We incubated the sections with these 'sandwiches' at 4°C overnight.

3.2.4 Semi-quantitative CHR-IHC analysis

Slides were scanned by Panoramic MIDI II (3DHISTECH Ltd.) scanner. Using Panoramic Viewer software (3DHISTECH Ltd.) we took randomly 10-10 photos at high magnification (400x). According to the spreading pattern of NFTs we focused on the transentorhinal and neocortical regions on aHPC and MFG samples, respectively. Semi-quantitative scoring was carried out with ImageJ software. 'Cell counter' module helped us to mark and count the differently labelled neurons based on a 4-grade intensity scale (0, 1+, 2+, 3+). We determined the mean IHC intensity scores for each case. Then mean intensity values were also calculated for aHPC and MFG region in early and late stages.

3.2.5 FDL-IHC digital image analysis

Fluorescent microscopy was executed as it was discussed in *3.1.5* subparagraph. 5-5 medium magnification (200x) images/cases were taken. Digital analysis of phospho-tau (green) and LMTK2 (red) fluorescent signals was performed with ImageJ software according to the followings: 1) Images with merged red and green channel data were opened in one 'stack'. The RGBs were converted into 8-bit greyscale images, but original red and green channel data were

kept in order to be able to redirect the measured greyscale intensities. 2) Thresholds were adjusted manually if needed. 3) Objects larger than 400 pixels were evaluated. Due to the redirecting method we acquired red and green channel row integrated density data columns relating to a given region of interest (ROI). According to the phospho-tau/LMTK2 relation we proposed that the sum of the fluorescent signals of the proteins can be considered invariable on the analysed images. We determined the percentage distribution of green and red fluorescent signals for each case. Then group-based comparison was also carried out by transforming these red and green channel data using the following equation:

$$R-G/R+G = X \quad (1)$$

, where R is the measured percentage intensity of red (LMTK2) signal, G is the measured percentage intensity of green (phospho-tau) signal and X can take value between (-1) and (+1). If X= (-1) 100% green and 0% red signal was measured, X= (+1) refers to 100%red and 0% green signals.

It is important to emphasise that CHR-IHC was performed to compare the mean LMTK2 intensity scores *between* the groups, while FDL-IHC measured the correlation between the percentage intensity of phospho-tau/LMTK2 signals *within* an experimental group.

3.2.6. Statistical tests

Since, CHR-IHC data followed normal distribution (Shapiro-Wilk test) mean semi-quantitative LMTK2 scores were evaluated with t-test between the experimental groups. Analysis of covariance (ANCOVA) was also run to test the effect of age, mini-mental state examination (MMSE) and apolipoprotein E (APOE) gene polymorphism on the CHR-IHC results. FDL-IHC data was not normally distributed, thus Spearman's correlation was applicated to measure the statistical significance of percentage distribution of phospho-tau/LMTK2 fluorescent signals.

4. Results

4.1 Neuropathological characterization of LMTK2 in AD and neocortical LBD

4.1.1 CHR-IHC results

LMTK2 immunolabelling located to the cytoplasm of neurons; glial cells and nuclei of neurons were negative. In AD the extracellular Aβ plaques were negative. The mean cytoplasmic LMTK2 immunopositivity was similarly weak in both tangle-bearing and morphologically normal cells. Differences between the IHC intensities of the experimental groups were obvious. Basically, LMTK2 immunopositivity was decreased in every cortical layer in AD compared to CNT and neocortical LBD groups.

4.2.1 IF-IHC results

1272 neurons were assessed altogether on the fluorescent images. Although, mean intensity of the cases varied within the groups (13.6-19 in CNT, 10.8-13.4 in AD and 12.8-16.4 in neocortical LBD cases) their standard deviations tend to be almost identical providing an adequate basis for statistical analysis. One-way ANOVA revealed statistically significant ($p<0.001$) difference among the mean greyscale intensities of the three experimental groups. Pairwise comparison showed significant alterations between CNT versus (vs.) AD ($p<0.001$) and neocortical LBD vs. AD ($p=0.014$) groups, while CNT vs. neocortical LBD comparison were not statistically relevant. According to ANCOVA neither age at death ($p=0.100$) nor post-mortem delay ($p=0.718$) significantly influenced the IF-IHC results.

4.2 Correlation between LMTK2 and tau-pathology

4.2.1 CHR-IHC results

We evaluated the intensities of 1215 neurons in the 4 experimental groups (aHPC and MFG regions in early and late neuropathological stages of AD). In the NFT-affected 3 groups (MFG in late and aHPC in both stages) the low LMTK2 intensity values (+1) dominated, while the most intense immunoreaction (3+) were detectable only in the endogenous control MFG region in early stage. IHC intensity scores of the cases varied within the experimental groups: 2.13-2.92 in early stage MFG, 1.07-1.70 in early stage aHPC, 1.22-1.81 in late stage MFG and 1.00-1.55 in late stage aHPC regions. Nevertheless, their standard deviations rendered an adequate basis for statistical analysis. Calculated mean intensity scores of the groups were the following: 2.59 in early stage MFG, 1.28 in early stage aHPC, 1.43 in late stage MFG and 1.24 in late

stage aHPC groups. Pairwise comparison revealed a significant alteration in the LMTK2 IHC intensity scores between endogenous control (MFG early stage) and the three NFT-affected regions (MFG in late and aHPC in both stages). Among the latter three groups we did not detected statistically significant difference. According to ANCOVA neither age (p=0.137), nor MMSE score (p=0.132), nor APOE polymorphism (p=0.253) influenced significantly the LMTK2 CHR-IHC results.

4.2.2 FDL-IHC results

Phospho-tau/LMTK2 FDL IHC showed LMTK2 predominance in the endogenous control region (MFG in early stage), while there was an obvious phospho-tau overburden and decreased LMTK2 signal in the NFT-affected regions (MFG in late and aHPC in both stages). Figure 1. depicts the percentage distribution of phospho-tau/LMTK2 signals for each case. Based on this data group level comparison of green (phospho-tau) and red (LMTK2) signals are presented on Figure 2. Statistical analysis of red (LMTK2) and green (phospho-tau) channel data revealed a strong negative correlation (Spearman Rank Order Correlation Coefficient = (-1)) within each experimental group.

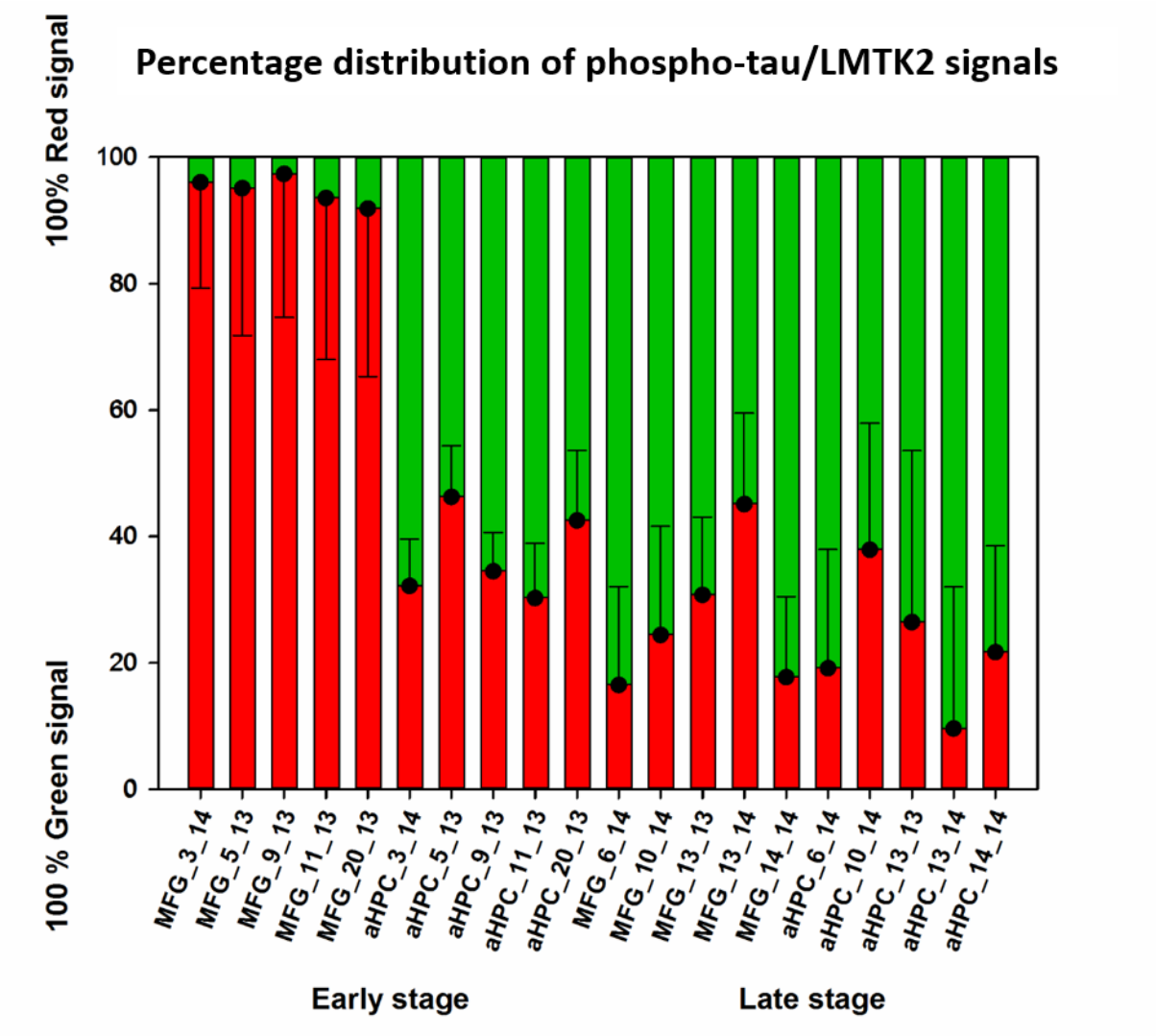

Figure 1. Bars depict the mean level (in %) of fluorescence for red (lemur tyrosine kinase-2 (LMTK2)) and green (phospho-tau) channels of images from the middle frontal gyrus (MFG) and anterior hippocampus (aHPC) in early and late neuropathological stages of Alzheimer's disease.

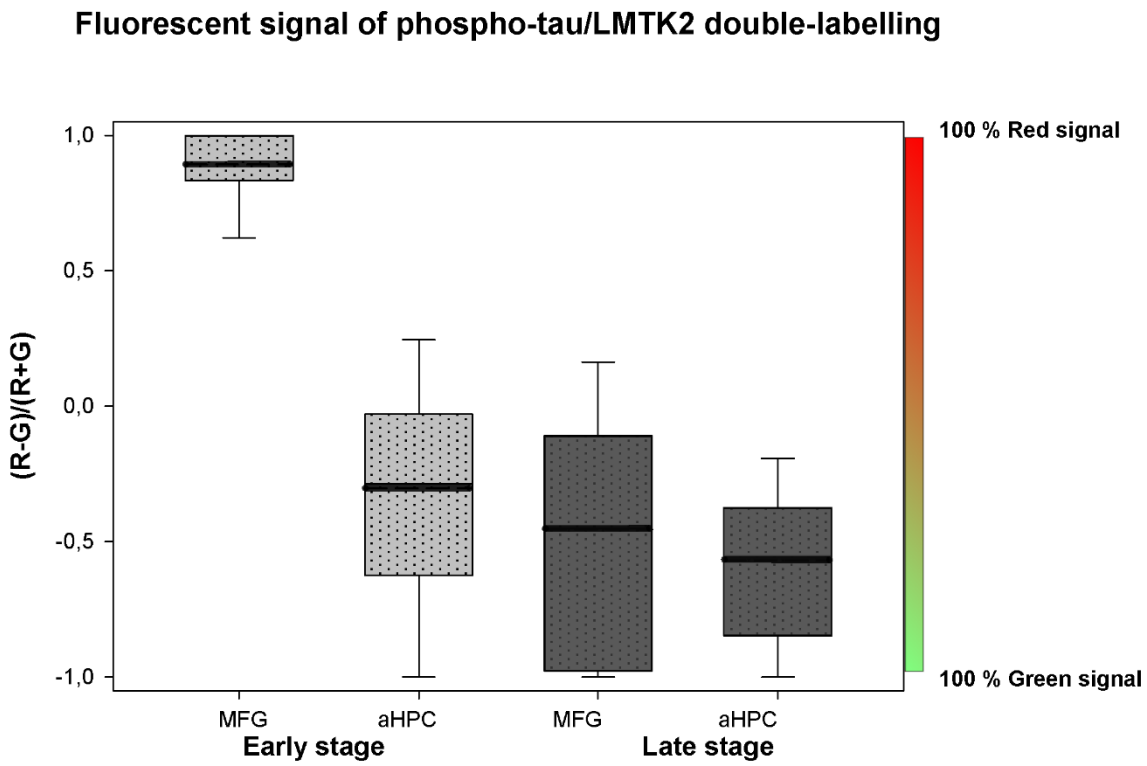

Figure 2. Phospho-tau and lemur tyrosine kinase 2 (LMTK2) double-labelling fluorescent immunohistochemistry signals of the middle frontal gyrus (MFG) and anterior hippocampus (aHPC) in early (dotted light gray boxes) and late (dotted dark gray boxes) neuropathological stages of Alzheimer's disease are quantified. Boxes represent the interquartile range of the fluorescence signal of phospho-tau (green) and LMTK2 (red) on a unified scale (-1 to +1) with median levels indicated by black lines. [-1 corresponds to 100% phospho-tau signal compared to 0% LMTK2; +1 means 100% LMTK2 signal and 0% phospho-tau].

5. Discussion

In accordance with the Human Protein Atlas LMTK2 CHR-IHC labelling localised to the cytoplasm of the neurons in both neurodegenerative and age-matched control groups; glial cells and nuclei of neurons were negative. Regarding AD-specific pathological changes there was no immunoreaction in the Aβ plaques proposing that LMTK2 is not involved in the formation of these protein aggregates. Tangle-bearing and morphologically normal neurons showed similarly week average cytoplasmic LMTK2 immunopositivity.

IF-IHC data revealed that the level of LMTK2 is significantly decreased in AD compared to CNTs and neocortical LBDs. Statistical tests showed significant alterations between AD vs. CNT and AD vs. neocortical LBD groups. Despite the subtle reduction measured in neocortical LBD group, the CNT vs. neocortical LBD comparison had no significant result. Based on ANCOVA neither post-mortem delay nor age ate death significantly influenced the IF-IHC data. The minimal decrease in the protein's level in neocortical LBDs probably resulted from the frequently observed coexisting AD-type pathology. This theory has been experimentally validated, suggesting that alteration of LMTK2 is specific to AD/tauopathies and it is not directly related to α-synucleinopathies.

LMTK2 CHR-IHC and phospho-tau/LMTK2 FDL-IHC confirmed that LMTK2 reduction is not a general feature of AD patients' brains, rather it significantly correlates with the extent of NFT pathology. LMTK2 immunopositivity was significantly higher between the NFT-spared MFG and highly affected aHPC brain regions even in the same early stage AD patients. Age, MSSE scores and APOE polymorphism did not influence significantly the LMTK2 CHR-IHC results. Statistical analysis of phospho-tau/LMTK2 signals revealed strong negative correlation between the regional distributions of the two protein. Consequently, LMTK2 expression is inversely proportionate to the extent of phospho-tau/NFT pathology.

Analogously to our results a few studies have also detected decreased LMTK2 level in AD. Genome-wide expression profiling found reduced LMTK2 expression in the neocortex and in the hippocampus of transgenic tau (Tau 301L) mice, while there was no difference in the NFT-spared cerebellum. Mórotz et al. in 2019 published a western blot study complementary to our IHC work (partially on the same patients). They established 3 experimental groups based on the Braak (tau) neuropathological staging: control – Braak I-II; mild dementia – Braak IV-V; severe dementia Braak V-VI). They reported decreased LMTK2 expression in the frontal cortex with the progression of dementia, while there was no alteration in NFT-spared cerebellum

(similarly to the animal model). However, they did not specify the investigated region(s) of the frontal cortex, moreover aHPC region was not evaluated, thus direct comparison to our work is not possible. Nevertheless, the NFT-dependent decrease of LMTK2 level, as well as the negative result in the NFT-spared cerebellum (which is represented by the endogenous control MFG region in early neuropathological stage in our experimental setting) provide a certain degree of validation to our study.

Although, the investigation of LMTK2 signalling was far beyond the scope of our studies, based on previous cell biological and animal model data we suggested three potential mechanism, which may contribute to neurodegeneration under pathological circumstances. Reduced LMTK2 level is implicated in 1) disruption of axonal transport; 2) tau hyperphosphorylation; 3) enhanced apoptosis.

Neuronal homeostasis requires well-organized, precise axonal transport. Any defect of this complex machinery may result in the accumulation of transported protein and subcellular organelles. According to the literature disruption of axonal transport is an early event in the pathogenesis of neurodegenerative disorders. Physiologically, LMTK2 is involved in the regulation of axonal transport. A recent study identified a direct interaction between LMTK2 and the light chains (KLC 1/2) of the major molecular motor protein Kinesin-1. This interaction facilitates the axonal transport of LMTK2, as well as induces the formation p35-LMTK2-KLC1 complex. siRNA silencing of LMTK2 disrupted the axonal transport of both p35 and CDK5. Owing to that CDK5 is essential for several neuronal functions, defect of its intracellular transport may contribute to neurodegenerative processes.

Furthermore, LMTK2 is involved also indirectly in the Kinsin-1-mediated axonal transport. Phosphorylation of KLCs is an important regulatory mechanism of cargo binding and release; one of the key molecules in this process is GSK3β. First prediction about the indirect regulatory link between CDK5 and GSK3β (via PP1C) was made in 2004. However, LMTK2 was identified eight years later, in 2012 as the missing link of the CDK/p35-PP1C-GSK3β signalling. The four proteins form a common phosphorylation pathway, which regulates the Kinesin-1-mediated axonal transport. CDK5/p35 activates LMTK2 by phosphorylating it on serine-1418. Phoshorylated-LMTK2 inhibits PP1C via a threonine-320 phosphorylation. Thus, PP1 cannot effectively remove the inhibitory phosphoryl groups from GSK3β serine-9. Inhibited GSK3β cannot phosphorylate KLC2, which in turn facilitates cargo binding to KLC2 (i.e. mothers against decapentaplegic homolog 2 (Smad2)). Consequently, LMTK2 is a positive regulator of Kinesin-1-mediated Smad2 transport via the inhibition of KLC2 phosphorylation.

Smad2 is key player of the transforming growth factor-β (TGFβ) nucleocytoplasmic signalling. LMTK2 knock-out disrupted the binding of Smad2 to KLC2 causing altered TGFβ signalling. Defected TGFβ/Smad2 signalling has been observed in common neurodegenerative diseases, including AD, which may confirm the role of LMTK2 in the pathomechanism.

NFTs are hallmark pathological features of AD. Major component of these protein aggregates is the hyperphosphorylated tau. CDK5 and GSK3β are well-known major tau kinases involved in tau hyperphosphorylation in vivo. Although, both CDK5 and GSK3β are sufficient for tau hyperphosphorylation, interestingly there is a negative regulatory link between the enzymes. As we described above CDK5 indirectly inhibits GSK3β, which is an age-dependent mechanism. GSK3β activity was significantly higher in aged mice compared to young animals. This alteration led to tau hyperphosphorylation. A possible explanation is the impairment of mechanisms inhibiting GSK3β (i.e. LMTK2 signalling). Physiologically, CDK5/p35 activates LMTK2. However, in AD neuronal stress results in calpain overactivation. These enzymes cleave p35 into p25 and p10. CDK5/p25 has prolonged half-life and activity contributing to tau hyperphosphorylation. p25 has lower binding-affinity to LMTK2 than p35, which may explain the decreased LMTK2 activity in AD. These changes cause PP1C disinhibition and indirectly GSK3β overactivation leading to tau hyperphosphorylation.

A recent siRNA-based high throughput screen study has identified LMTK2 as a potential apoptosis regulator. LMTK2 gene silencing decreased the levels of anti-apoptotic 'B-cell lymphoma-2' (Bcl-2) and 'B-cell lymphoma-extra-large' (Bcl-xL) and increased the level of pro-apoptotic 'Bcl-2-interacting mediator of cell death' (Bim). Treated cells had increased sensitivity to apoptosis-inducing and other cytotoxic agents. Elevated Bim and decreased Bcl-2 and Bcl-xL levels resulted from the missing LMTK2-mediated inhibition on PP1 and GSK3β. In AD patient's brain the Bim level is higher, while Bcl-2 is probably protective against AD-related noxae. Thereby, LMTK2 has an important role in the regulation of apoptosis, whereas its decreased activity may contribute to neuronal loss in neurodegenerative disorders.

According to our knowledge majority of neurons are terminally differentiated cells. However, certain noxious stimuli (i.e. oxidative stress, Aβ peptides, hyperphosphorylated tau) can induce aberrant cell-cycle reactivation. Since, these cells lost their proliferative capacity, cell-cycle re-entry resulted in apoptosis by different regulatory mechanisms. Group of researchers consider neurodegeneration as the 'cancer of neurons'. It is possible that noxious factors which cause uncontrolled proliferation in other tissues, resulted in degenerative changes and apoptotic cell loss in neural tissue. Several studies reported decreased LMTK2 expression in malignant

tumours, suggesting that LMTK2 acts as a tumour-suppressor protein. Cell-cycle reactivation facilitates cyclin D and cyclin E expression as well as triggers the activity of G_1 and G_2 phase kinases. CDK activity causes the phosphorylation of retinoblastoma protein and accompanying E2F release. E2F supresses the expression of pro-apoptotic genes and transactivates downstream cell-cycle genes leading to the progression of this ultimately lethal cycle. Considering LMTK2 as a cell-cycle inhibitor/tumour-suppressor protein it is possible that E2F decreases the expression of LMTK2 by transcriptional silencing. However, the connection between LMTK2 and E2F remains to be proven.

Short summary:

- LMTK2 is localised to neuronal cytoplasm in both neurodegenerative disorders (AD, neocortical DLB) and non-demented age-matched controls by CHR-IHC

- Regarding AD-specific pathological changes Aβ plaques are negative, tangle-bearing and morphologically normal neurons showed similarly weak average cytoplasmic LMTK2 immunopositivity.

- LMTK2 immunolabelling intensity was significantly decreased in severe AD (Braak VI) compared to neocortical DLB and CNT groups by IF-IHC. This tendency was observed in every cortical layer.

- LMTK2 CHR-IHC intensity scores were significantly decreased in the NFT-affected aHPC region in early neuropathological stage of AD as well as in both MFG and aHPC regions in late neuropathological stage of AD compared to the NFT-spared endogenous control MFG region in early neuropathological stage of AD

- Phospho-tau/LMTK2 FDL-IHC revealed strong negative correlation between the regional distribution of the proteins in early and late neuropathological stages of AD. Consequently, the expression of LMTK2 is inversely proportionate to the extent of phospho-tau/NFT pathology. LMTK2 reduction is not a generalized feature of AD patients' brains, rather it is strongly associated to NFTs.

Probably, LMTK2 has an important role in the pathomechanism of AD. We believe that it will be a potential biomarker/drug target in the future. Recent studies have confirmed this hypothesis. The LMTK2 overexpression had significant neuroprotective effect in cerebral ischemia/reperfusion model in vitro. It is well-known that coexisting vascular pathology

facilitates the severity of AD symptoms, therefore pharmacological manipulation of LMTK2 level could be beneficial in AD. In accordance with this a paper described a 2-O-Tetradecanoylphorbol-13-acetate (TPA) response element in the promoter region of LMTK2 gene. The synthetic Protein Kinase C activator TPA increased the expression of LMTK2. Nevertheless, further comprehensive analysis on the protein is needed to elucidate LMTK2's role in neurodegeneration and as a therapeutic target in AD.

6. Summary

Alzheimer's disease (AD) and dementia with Lewy bodies (DLB) are the most common neurodegenerative dementias affecting millions of people worldwide. According to our knowledge the diseases are incurable, only supportive therapy available. Therefore, there is a growing pressure on the scientists to provide novel therapeutic targets by mapping the pathomechanism of the diseases. Lemur tyrosine kinase 2 has become to the centre of interest, recently. Cell biological and animal model studies suggest that the enzyme is implicated in neurodegeneration. However, the number of human-based investigations are very limited.

In our work we aimed the neuropathological characterization of LMTK2 in the two most frequent neurodegenerative dementias, as well as the clarification of the proposed link between LMTK2 and tau pathology.

Neuropathological characterization of LMTK2 was carried out on post-mortem brain samples of AD, clinically DLB, histologically neocortical Lewy body disease (LBD) patients, compared them to age-matched controls (CNTs) without dementia. For morphometric evaluation chromogenic (CHR) immunohistochemistry (IHC) was used. Group-based comparison of LMTK2 immunopositivity was performed with fluorescent IHC. LMTK2-tau correlation was observed on early (Braak I-III.) and late (Braak VI.) AD neuropathological stage samples from the region of anterior hippocampus (aHPC) and middle frontal gyrus (MFG) with LMTK2 CHR-IHC and phospho-tau/LMTK2 fluorescent double labelling IHC techniques.

LMTK2 is a neuron-specific marker. Immunolabelling localized to the cytoplasm on both neurodegenerative and CNT samples. Regarding hallmark pathological features of AD, amyloid-β plaques were negative, neurofibrillary tangle (NFT)-bearing neurons and morphologically normal cells showed similarly weak average cytoplasmic immunoreaction. In AD the LMTK2 immunopositivity was significantly decreased compared to neocortical LBD and CNT group. This tendency was observed in every cortical layer. We detected a strong negative correlation between phospho-tau and LMTK2 signals in different neuropathological stages of AD.

According to our results decreased level of LMTK2 is specific to AD. The alteration is not a general features of AD brains, because it is inversely proportionate to the extent of NFT pathology. We believe that our research can contribute to the understanding of LMTK2's role in neurodegeneration and the protein will be a potential biomarker/drug target in AD.

7. Acknowledgements

I would like to thank to my supervisors **Prof. Tibor Hortobágyi** and **Prof. Dag Aarsland** for guiding me into scientific life, familiarizing me with research work and supporting my career development by their expertise and precious advices.

I am grateful to the head of Institute of Pathology **Prof. Gábor Méhes** and the head of MTA-DE Cerebrovascular and Neurodegenerative Research Group **Prof. László Csiba** for their support and for providing the conditions for my research work.

Special thanks to the employees of Laboratory of Neuropathology and Laboratory of Institute of Pathology, especially to **Katalin Nagy** and **Henrietta Kiss** for their assistance during the experiments.

Also, many thanks to **Máté Szarka** and the team of Vitrolink for their invaluable help with digital images analysis and data processing.

Finally, I would like to express my gratitude to **Gábor Mórotz** and **Prof. Chris Miller** for discussions about LMTK2, to **Orsolya Matolay** for her assistance with slide scanning and fluorescent microscopy, and to all of my co-authors and former colleagues for contributing to my PhD work.

8. Funding

Supported by the ÚNKP-17-3 and ÚNKP-18-3 New National Excellence Program of the Ministry of Human Capacity and ÚNKP-19-3 New National Excellence Program of the Ministry of Innovation and Technology, Hungarian Brain Research Program (NAP_KTIA_13_NAP-A-II/7 és 2017-1.2.1-NKP-2017-00002), AGR_PIAC_13-1-2013-0008, NKFIH-SNN-132999, GINOP-2.3.2-15-2016-00043, EFOP-3.6.3-VEKOP-16-2017-00009, MTA-DE Cerebrovascular and Neurodegenerative Research Group and DE ÁOK Research Fund.

9. Appendix

UNIVERSITY AND NATIONAL LIBRARY
UNIVERSITY OF DEBRECEN
H-4002 Egyetem tér 1, Debrecen
Phone: +3652/410-443, email: publikaciok@lib.unideb.hu

Registry number: DEENK/20/2020.PL
Subject: PhD Publikációs Lista

Candidate: János Bencze
Neptun ID: WD33S7
Doctoral School: Doctoral School of Neurosciences

List of publications related to the dissertation

1. **Bencze, J.**, Szarka, M., Bencs, V., Szabó, R. N., Módis, L. V., Aarsland, D., Hortobágyi, T.: Lemur tyrosine kinase 2 (LMTK2) level inversely correlates with phospho-tau in neuropathological stages of Alzheimer's disease.
Brain Sci. 10 (2), 1-14, 2020.
IF: 2.786 (2018)

2. **Bencze, J.**, Szarka, M., Bencs, V., Szabó, R. N., Smajda, M., Aarsland, D., Hortobágyi, T.: Neuropathological characterization of Lemur tyrosine kinase 2 (LMTK2) in Alzheimer's disease and neocortical Lewy body disease.
Sci. Rep. 9 (1), 1-9, 2019.
DOI: https://doi.org/10.1038/s41598-019-53638-9
IF: 4.011 (2018)

List of other publications

3. Gergely, P., Murnyák, B., **Bencze, J.**, Kurucz, A., Varjas, T., Gombos, K., Hortobágyi, T.: Tyrosine kinase inhibitor Imatinib mesylate alters DMBA-induced early onco/suppressor-gene expression with tissue-specificity in mice.
Biomed. Res. Int. 2019, 1-12, 2019.
IF: 2.197 (2018)

4. **Bencze, J.**, Mórotz, M. G., Woosung, S., Bencs, V., Kálmán, J., Miller, C. C. J., Hortobágyi, T.: Biological function of Lemur tyrosine kinase 2 (LMTK2): implications in neurodegeneration.
Mol. Brain. 11 (20), 1-9, 2018.
DOI: https://doi.org/10.1186/s13041-018-0363-x
IF: 4.051

5. **Bencze, J.**, Pocsai, K., Murnyák, B., Gergely, P., Juhász, B., Szilvássy, Z., Hortobágyi, T.: The melanin-concentrating hormone system in human, rodent and avian brain.
Open Med. 13 (1), 264-269, 2018.
DOI: http://dx.doi.org/10.1515/med-2018-0040
IF: 1.221

6. **Bencze, J.**, Simon, V., Bereczki, E., Laczkóné Majer, R., Varkoly, G., Murnyák, B., Kálmán, J., Hortobágyi, T.: A Lewy-testes demencia klinikai és neuropatológiai jellemzői.
Orvosi Hetilap. 158 (17), 643-652, 2017.
DOI: http://dx.doi.org/10.1556/650.2017.30735
IF: 0.322

7. Kovács, G. G., Xie, S. X., Lee, E. B., Robinson, J. L., Caswell, C., Irwin, D. J., Toledo, J. B., Johnson, V. E., Smith, D. H., Alafuzoff, I., Attems, J., **Bencze, J.**, Bieniek, K. F., Bigio, E. H., Bódi, I., Budka, H., Dickson, D. W., Dugger, B. N., Duyckaerts, C., Ferrer, I., Forrest, S. L., Gelpi, E., Gentleman, S., Giaccone, G., Grinberg, L. T., Halliday, G., Hatanpaa, K. J., Hof, P. R., Hofer, M., Hortobágyi, T., Ironside, J. W., King, A., Kofler, J., Kővári, E., Kril, J. J., Love, S., Mackenzie, I. R., Mao, Q., Matej, R., McLean, C., Munoz, D. G., Murray, M. E., Neltner, J., Nelson, P. T., Ritchie, D., Rodriguez, R. D., Rohan, Z., Rozemuller, A., Sakai, K., Schultz, C., Seilhean, D., Smith, V., Tacik, P., Takahashi, H., Takao, M., Thal, D. R., Weis, S., Wharton, S. B., White III, C. L., Woulfe, J. M., Yamada, M., Trojanowski, J. Q.: Multisite Assessment of Aging-Related Tau Astrogliopathy (ARTAG).
J. Neuropathol. Exp. Neurol. 76 (7), 605-619, 2017.
IF: 3.49

8. Hortobágyi, T., **Bencze, J.**, Murnyák, B., Kouhsari, M. C., Bognár, L., Marko-Varga, G.: Pathophysiology of meningioma growth in pregnancy.
Open Med. 12, 195-200, 2017.
IF: 0.484

9. Varkoly, G., **Bencze, J.**, Hortobágyi, T., Módis, L.: A corneális sebgyógyulás és az extracelluláris mátrix.
Orvosi Hetilap. 157 (25), 995-999, 2016.
DOI: http://dx.doi.org/10.1556/650.2016.30475
IF: 0.349

10. Csonka, T., Murnyák, B., Szepesi, R., **Bencze, J.**, Bognár, L., Klekner, Á., Hortobágyi, T.: Assessment of candidate immunohistochemical prognostic markers of meningioma recurrence.
Folia Neuropathol. 54 (2), 114-126, 2016.
IF: 1.093

UNIVERSITY of DEBRECEN

UNIVERSITY AND NATIONAL LIBRARY
UNIVERSITY OF DEBRECEN
H-4002 Egyetem tér 1, Debrecen
Phone: +3652/410-443, email: publikaciok@lib.unideb.hu

11. Varkoly, G., **Bencze, J.**, Módis, L., Hortobágyi, T.: Az extracelluláris mátrix rendellenességei epithelialis-stromalis és stromalis cornealis dystrophiákban.
Orvosi Hetilap. 157 (33), 1299-1303, 2016.
DOI: http://dx.doi.org/10.1556/650.2016.30481
IF: 0.349

12. **Bencze, J.**, Varkoly, G., Hortobágyi, T.: Meningeoma és terhesség.
Ideggyogy. Szle. 69 (7-8), 220-224, 2016.
DOI: http://dx.doi.org/10.18071/isz.69.0220
IF: 0.322

13. Hortobágyi, T., **Bencze, J.**, Varkoly, G., Kouhsari, M. C., Klekner, Á.: Meningioma recurrence.
Open Med. 11 (1), 168-173, 2016.
DOI: http://dx.doi.org/https://doi.org/10.1515/med-2016-0032
IF: 0.294

Total IF of journals (all publications): 20,969
Total IF of journals (publications related to the dissertation): 6,797

The Candidate's publication data submitted to the iDEa Tudóstér have been validated by DEENK on the basis of the Journal Citation Report (Impact Factor) database.

30 January, 2020